Chinese Chemical Letters 33 (2022) 293–297

Contents lists available at ScienceDirect

Chinese Chemical Letters

journal homepage: www.elsevier.com/locate/cclet

MoS_2 nanosheets and bulk materials altered lipid profiles in 3D Caco-2 spheroids

Min Xie[a,b,c], Chaobo Huang[b], Yongqi Liang[c], Shuang Li[c], Liping Sheng[a,*], Yi Cao[d,*]

[a] National Local Joint Engineering Laboratory for New Petro-chemical Materials and Fine Utilization of Resources, College of Chemistry and Chemical Engineering, Hunan Normal University, Changsha 410081, China
[b] College of Chemical Engineering, Nanjing Forestry University (NFU), Nanjing 210037, China
[c] Key Laboratory of Environment-Friendly Chemistry and Applications of Ministry Education, Laboratory of Biochemistry, College of Chemistry, Xiangtan University, Xiangtan 411105, China
[d] Hunan Province Key Laboratory of Typical Environmental Pollution and Health Hazards, School of Public Health, University of South China, Hengyang 421001, China

ARTICLE INFO

Article history:
Received 20 April 2021
Revised 16 May 2021
Accepted 18 June 2021
Available online 26 June 2021

Keywords:
MoS_2 nanosheets (NSs)
3D Caco-2 spheroids
Transcriptomics
Lipidomics
Fat digestion and absorption (map04975)

ABSTRACT

MoS_2 nanosheets (NSs) are novel 2D nanomaterials (NMs) with potential uses in many areas, and therefore oral exposure route to MoS_2 NSs is plausible. Currently, MoS_2 NSs are considered as biocompatible NMs, but there is lacking of systemic investigations to study the interactions of MoS_2 NSs with intestinal cells. In this study, we exposed the 3D Caco-2 spheroids to MoS_2 NSs or MoS_2 powders (denoted as MoS_2-bulk), and investigated the potential adverse effects of MoS_2-materials based on transcriptomics and lipidomics analysis. As expected, both MoS_2 NSs and MoS_2-bulk were dose-dependently internalized into 3D Caco-2 spheroids but did not induce cytotoxicity, membrane disruption or decrease of thiols. However, the Gene Ontology (GO) and Kyoto Encyclopedia of Gene and Genomes (KEGG) analysis indicated that nutrient absorption and metabolism was decreased. One of the most significantly decreased KEGG pathways is fat digestion and absorption (map04975), and Western blotting analysis further showed that fatty acid binding protein 1 and apolipoprotein A1, key proteins involved in fat digestion and absorption, were down-regulated by MoS_2 NSs or MoS_2-bulk. In addition, BODIPY 493/503 staining suggested that exposure to MoS_2 NSs and MoS_2-bulk decreased lipid levels in the spheroids. However, lipidomics data indicated that MoS_2 materials only decreased 8 lipid classes, including lysophosphatidylcholine, lysodimethylphosphatidylethanolamine, *N*-acylethanolamine, ceramide phosphoethanolamines, gangliosides, lysosphingomyelin and sulfatide, whereas most of the lipid classes were indeed increased. In addition, MoS_2 NSs was more potent to decrease the lipid classes compared with MoS_2-bulk. Combined, the results from this study showed that MoS_2 NSs and bulk materials were non-cytotoxic but altered lipid profiles in 3D Caco-2 spheroids.

Graphene-based nanomaterials (NMs) are magic 2D materials with great uses in many different areas, ranging from environmental protection to biotechnology [1,2]. Due to the success of graphene-based NMs, the development of 2D NMs based on other materials has gained extensive interest. MoS_2 nanosheets (NSs) share some similarities with graphene-based NMs, for example, large surface area and absorbance in near-infrared region, and thus MoS_2 NSs have been explored as promising 2D materials particularly for biomedical applications, including but not limited to drug delivery, biomedical imaging and bio-sensing [3,4]. However, the toxic effects of MoS_2 NSs should still be carefully evaluated.

At present, MoS_2 NSs are generally considered as materials with relatively low toxicity [3,4]. For example, studies by using *in vitro* models showed that MoS_2 NSs were not cytotoxic to normal mammalian cells [5,6], or only modestly toxic at relatively high concentrations [7,8]. Under *in vivo* conditions, administration of MoS_2 NSs into mice *via* different routes did not lead to obvious toxicological outcomes, and the materials were rapidly excreted *via* feces and urine [9,10]. However, a recent study showed that MoS_2 NSs induced oxidative stress mediated toxicity in Asian weaver ants [11]. This suggests a need to evaluate the possible toxicity of MoS_2 NSs by different models. On the other hand, even NMs with no obvious cytotoxicity might induce other toxic effects. For instance, a

* Corresponding authors.
E-mail addresses: sleeping1217@126.com (L. Sheng), caoyi39@126.com (Y. Cao).

https://doi.org/10.1016/j.cclet.2021.06.049
1001-8417/

recent study showed that graphene quantum dots at non-cytotoxic concentrations induced genotoxic response in macrophages [12]. Recently, we reported that Au nanorods [13] and Ti-based NMs [14,15] were not cytotoxic to human endothelial cells but disrupted NO signaling pathway due to an effect on the transcription factors Kruppel-like factors (KLFs). Indeed, some types of NMs at non-cytotoxic concentrations have been shown to induce adverse health effects by the dysfunction of KLFs [16]. Hence, it is necessary to systemically investigate the changes of signaling pathways induced by NM exposure, even if the NMs have no cytotoxicity.

Generally, traditional toxicology studies focused on a specific signaling pathway but failed to investigate the systemic changes. The advances in omics-technologies, such as transcriptomics, metabolomics and lipidomics, provide an opportunity to systemically investigate the adverse effects of NMs [17]. In this study, we evaluated the adverse effects of MoS_2 NSs to 3D Caco-2 spheroids based on transcriptomics and lipidomics analysis. We used 3D Caco-2 spheroids as the model for intestine, because the potential uses of NMs in biomedicine could result in the exposure of NMs to intestine, and 3D spheroids have been considered as advanced *in vitro* models to better predict the toxicological responses of tissues or organs compared with 2D conventional cell cultures [18]. Recently, we showed that 3D Caco-2 spheroids could be used to evaluate the interactions between TiO_2 nanoparticles (NPs) and intestinal cells [19]. The model was exposed to up to 128 μg/mL MoS_2 NSs or MoS_2 powders (denoted as MoS_2-bulk in this study) for 24 h. Because MoS_2 NSs is relatively new and there is currently lacking of report about the exposure levels of MoS_2 NSs to human beings, we used concentrations comparable to previous *in vitro* studies which investigated the toxicity of MoS_2 NSs [3,4]. After exposure, cytotoxicity was measured by acridine orange (AO) and 4′,6-diamidino-2-phenylindole (DAPI) counterstaining. Membrane integrity was indicated by the measurement of lactate dehydrogenase (LDH) release. Oxidative stress was indicated by the measurement of thiols. The interaction between materials and 3D Caco-2 spheroids was investigated by the measurement of intracellular Mo elements by inductively coupled plasma-mass spectrometry (ICP-MS). Afterwards, we exposed 3D Caco-2 spheroids to 32 μg/mL materials, and performed transcriptomics analysis to investigate the global gene expression profiles. The Gene Ontology (GO) and Kyoto Encyclopedia of Gene and Genomes (KEGG) analysis were used to indicate the changes of signaling pathways. Because the results suggested that MoS_2-materials affected fat digestion and absorption (see the results below), we also investigated the changes of lipids by BODIPY 493/503 staining and lipidomics.

The MoS_2 NSs and MoS_2-bulk materials were purchased from Nanjing XFNANO Materials Tech Co., Ltd. (code XF134) and Aladdin (Shanghai, China), respectively, and thoroughly characterized in this study. The Raman spectra (Fig. S1A in Supporting information) of MoS_2 NSs showed two peaks located at 383 cm^{-1} and 408 cm^{-1}, corresponding to in-plane E_2g peak and out-of-plane A_1g peak. The difference between the two peaks is 25 cm^{-1}, which could confirm the presence of monolayer of MoS_2 NSs. MoS_2-bulk depicted similar in-plane E_2g peak and out-of-plane A_1g peak as MoS_2 NSs (data not shown), indicating the same composition of these materials. The transmission electron microscope (TEM) image (Fig. S1B in Supporting information) confirmed the sheet-like structure of MoS_2 NSs. The inserted high resolution transmission electron microscope (HRTEM) image of clearly revealed the lattice fringe spacing of 0.6 nm, which agreed well with the (002) plane of MoS_2. The representative scanning electron microscopic (SEM) images indicated that MoS_2-bulk was also sheet-like but much larger in size compared with MoS_2 NSs (Figs. S2A and B in Supporting information). The atomic force microscope (AFM) images suggested that the thickness of MoS_2 NSs and MoS_2-bulk were approximately 3 nm (Fig. S1C in Supporting information) and 1.5 μm (Fig. S2C in Supporting information), respectively. The distribution of hydrodynamic size and zeta potential of MoS_2 NSs in water and medium was shown in Supplemental Fig. S3 (Supporting information). Both in water and medium, MoS_2 NSs had average hydrodynamic sizes larger than 300 nm and negative zeta potential. Meanwhile, the average polydispersity index (PDI) slightly increased from ~0.37 in water to ~0.46 in medium (Table S1 in Supporting information). The hydrodynamic size and zeta potential of MoS_2-bulk were not further measured in this study.

According to the representative AO/DAPI counterstaining images (Fig S4 in Supporting information), only few cells in the control (Fig. S4A), MoS_2 NS-exposed (Figs. S4C-E) and MoS_2-bulk-exposed groups (Figs. S4F-H) were stained by DAPI with blue fluorescence (correlating to dead cells). In addition, most of the cells of these groups were intact with round morphologies. The cellular viability was higher than 95% in control (Fig. S4A) and material-exposed spheroids (Figs. S4C-H). In contrast, short-term exposure to 1% Triton-X decreased the cellular viability to 75.4% (Fig. S4B). The results from LDH assay further showed that exposure to MoS_2 NSs or MoS_2-bulk did not significantly induce LDH release (Fig. S5 in Supporting information). The representative thiol measurement images (Fig. S6 in Supporting information) showed that most of the cells in control (Fig. S6A), MoS_2 NS-exposed (Figs. S6B-D) and MoS_2-bulk-exposed groups (Figs. S6E-G) were stained with blue fluorescence by VitaBright-48^{TM} (VB-48^{TM}) due to the presence of high levels of thiols. Quantitative analysis (Fig. S7 in Supporting information) suggested that compared with control (Fig. S7A), the percentage of cells in Q1lr, corresponding to cells with high levels of thiols, was not decreased after exposure to various concentrations of MoS_2 NSs (Figs. S7B-D) or MoS_2-bulk (Figs. S7E-G).

The above data obtained by AO/DAPI staining, LDH assay and thiol measurement suggested that MoS_2 NSs or MoS_2-bulk did not induce cytotoxicity or oxidative stress, indicating the high biocompatibility of MoS_2 materials. Typical NSs such as graphene oxide [20,21], BN NSs [22] and Mxene [23,24] have been shown to induce oxidative stress and/or disruption of membrane integrity in different *in vitro* models. For MoS_2 NSs, some studies found that only high levels of MoS_2 NSs could induce oxidative stress and membrane damages, but these effects were generally more modest compared with other NSs such as graphene-based materials [7,8]. The lack of acutely cytotoxic effects could also be because we used spheroid-based models, and tissue-cultures as advanced *in vitro* models may be more resistant to material exposure compared with 2D conventional cell cultures [18,25–27]. However, we did not further use 2D conventional cell cultures to compare the responses. Nonetheless, the results from this study suggested that MoS_2 materials at the tested concentrations were not cytotoxic to 3D Caco-2 spheroids.

The results from ICP-MS (Fig. S8 in Supporting information) indicated a dose-dependent increase of Mo elements in treated cells. However, MoS_2-bulk more effectively increased cellular Mo elements compared with MoS_2 NSs at the same mass concentrations. One possible explanation for this phenomenon is that the morphologies influenced the internalization of materials [28,29]. For example, we recently showed that nano-sized carbon black particles were internalized into macrophages with a relatively large amount, whereas the internalization of graphene oxide was negligible [30]. Another possibility is that MoS_2 NSs might be rapidly exported, and MoS_2 NSs administrated into mice could be rapidly excreted *via* feces and urine [9,10].

Despite no cytotoxicity, transcriptomics data suggested that both types of materials significantly altered transcriptome profiles. The Venn diagram (Fig. S9 in Supporting information) indicated that among the significantly changed genes, total of 5695 genes were altered by both types of materials, 160 genes were uniquely altered by MoS_2 NSs, and 1993 genes were uniquely altered by

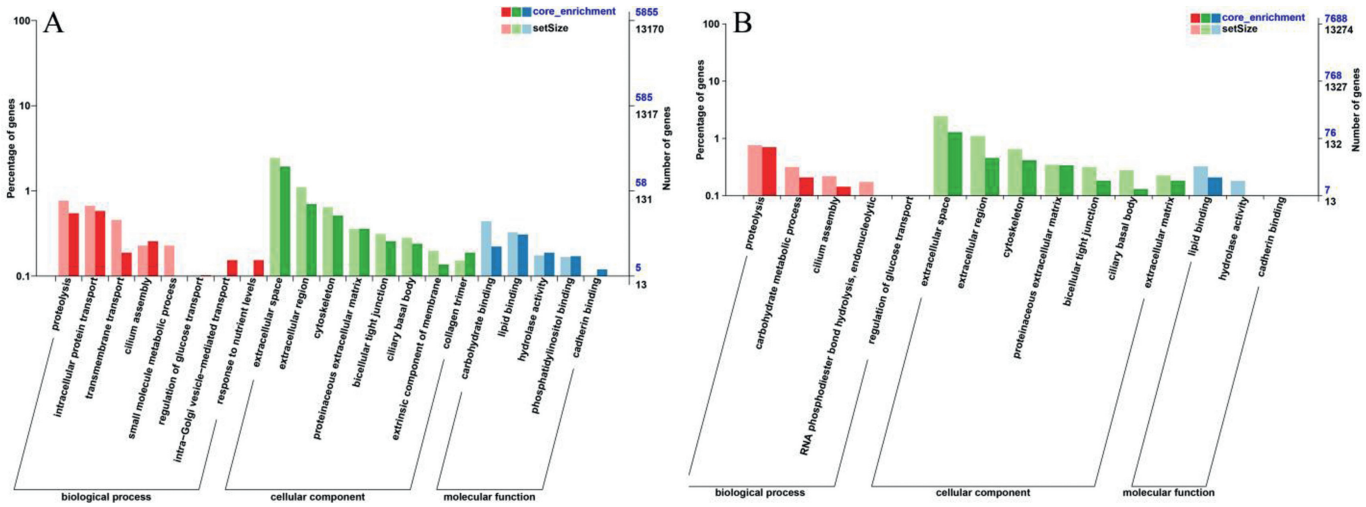

Fig. 1. GO enrichment. 3D Caco-2 spheroids were incubated with cell culture medium (control), 32 μg/mL MoS_2 NSs or MoS_2-bulk for 24 h. After exposure, transcriptomics was done. The significantly enriched GO terms were categorized to biological processes, cellular components and molecular functions, respectively. (A) The influence of MoS_2 NSs on GO terms. (B) The influence of MoS_2-bulk on GO terms.

MoS_2-bulk. The volcano plots showed that exposure to MoS_2 NSs led to totally 3414 significantly up-regulated genes and 2441 significantly down-regulated genes (Fig. S10A in Supporting information), whereas exposure to MoS_2-bulk led to totally 4176 significantly up-regulated genes and 3512 significantly down-regulated genes (Fig. S10B in Supporting information), respectively. These results suggested that MoS_2-bulk had greater impact on gene expression profiles compared with MoS_2 NSs. However, there were also genes that were uniquely altered by MoS_2 NSs. The volcano plot (Fig. S10C in Supporting information) indicated that compared with MoS_2 NS-exposed spheroids, exposure to MoS_2-bulk led to totally 196 significantly up-regulated genes and 44 significantly down-regulated genes. The corresponding top 10 significantly down-regulated and top 10 significantly up-regulated genes were shown in Tables S2 and S3 (Supporting information), respectively, and the top differentially changed GO terms and KEGG pathways were shown in Figs. S11 and S12 (Supporting information) (control MoS_2 NS-exposed spheroids, case MoS_2-bulk-exposed spheroids). These results could indicate a difference between 2D and bulk materials, but we did not further investigate the exact different responses induced by MoS_2 NSs and MoS_2-bulk.

Previously we reported that carbon nanotubes changed genes, GO terms and KEGG pathways related with cell death [31]. But in this study, we did not find similar effects, consistent with the non-cytotoxic profiles of MoS_2 materials. Therefore, we focused on the changes of other signaling pathways. We noticed that some significantly enriched GO terms could be related with nutrient absorption and metabolism. For example, the GO terms small molecule metabolic process (GO:0,044,281; $P = 0.0075$), proteinaceous extracellular matrix (GO:0,005,578; $P = 0.015$) and hydrolase activity (GO:0,016,787; $P = 0.031$) were significantly down-regulated by MoS_2 NSs (Fig. 1A). Similarly, MoS_2-bulk significantly down-regulated the GO terms carbohydrate metabolic process (GO:0,005,975; $P = 0.0073$), proteinaceous extracellular matrix (GO:0,005,578; $P = 0.0466$) and lipid binding (GO:0,008,289; $P = 0.0037$; Fig. 1B).

Consistently, KEGG pathways related with nutrient metabolism, biosynthesis and degradation were also significantly impaired by both types of materials. For example, MoS_2 NSs significantly down-regulated tyrosine metabolism (map00350; $P = 0.0257$), arginine biosynthesis (map00220; $P = 0.0049$) and protein digestion and absorption (map04974; $P = 0.045$; Fig. 2A). These effects were also observed in MoS_2-bulk-exposed spheroids (Fig. 2B).

Previously we suggested that exposure to NMs might affect nutrient absorption [32]. Some studies indicated that typical NMs including TiO_2, ZnO and SiO_2 NPs impaired nutrient absorption in a co-culture model based on Caco-2 cells due to the damages to absorptive microvilli [33–35]. In mice, Chen *et al.* also found that TiO_2 NPs impaired glucose transport due to the remodeling of the intestinal villi [36]. Interestingly, recent studies by investigating the global gene expression profiles also supported that NPs could affect nutrient metabolism. For instance, Türkez *et al.* showed that B_4C NPs affected the amino acid bio-synthesis pathway in human primary alveolar epithelial cells [37]. In another study, Tian *et al.* revealed that TiO_2 NPs activated the insulin signaling pathway and improved the metabolism of proteins, fats, and carbohydrates in silkworms [38]. We reported recently that graphene oxide altered lipid metabolism pathways in human endothelial cells, and this effect was correlated with the cytotoxicity of graphene oxide [39]. Combined with previous findings and our current observations, it appears that impaired nutrient transport is a common phenomenon after NM exposure

Of all the significantly decreased KEGG terms, we noticed that the KEGG term fat digestion and absorption (map04975) was significantly down-regulated by both MoS_2 NSs ($P = 0.00257$) and MoS_2-bulk ($P = 0.00296$). Fig. S13 (Supporting information) summarized the influence of materials on map04975, with the significantly down-regulated genes marked with green color. The heatmap based on transcriptomics data clearly indicated that MoS_2 NSs and MoS_2-bulk down-regulated key genes related with map04975 (Fig. 3A). Western blotting analysis further showed that the protein levels of fatty acid binding protein 1 (FABP1; Figs. 3B and C) were only significantly down-regulated by MoS_2-bulk ($P < 0.01$), whereas apolipoprotein A1 (APOA1; Figs. 3B and D) were decreased by both MoS_2 NSs and MoS_2-bulk ($P < 0.01$).

To confirm the influence of MoS_2 materials on lipids, we did lipid staining by using lipid-specific probe BODIPY493/503. The representative images suggested that the cells could be stained by BODIPY 493/503 with green color, but the staining appeared to be partially lost after exposure to MoS_2 NSs (Fig. S14B in Supporting information) or MoS_2-bulk (Fig. S14C in Supporting information) compared with control (Fig. S14A in Supporting information). A modest decrease of BODIPY 493/503 intensity was observed in MoS_2 NSs or MoS_2-bulk exposed cells (Fig. 4A). Hence, it is possible that MoS_2-materials decreased lipid contents in 3D spheroids as a possible consequence due to impaired fat absorption. It should

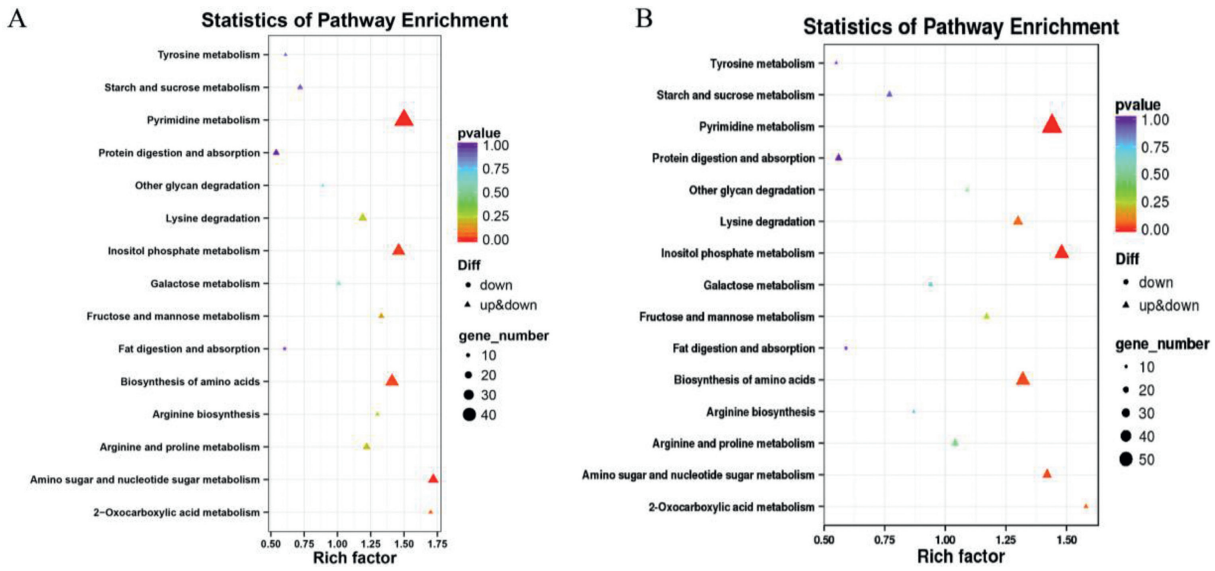

Fig. 2. KEGG enrichment. The significantly enriched KEGG terms related with nutrient biosynthesis, metabolism and degradation were categorized. (A) The influence of MoS_2 NSs on KEGG pathways. (B) The influence of MoS_2-bulk on KEGG pathways.

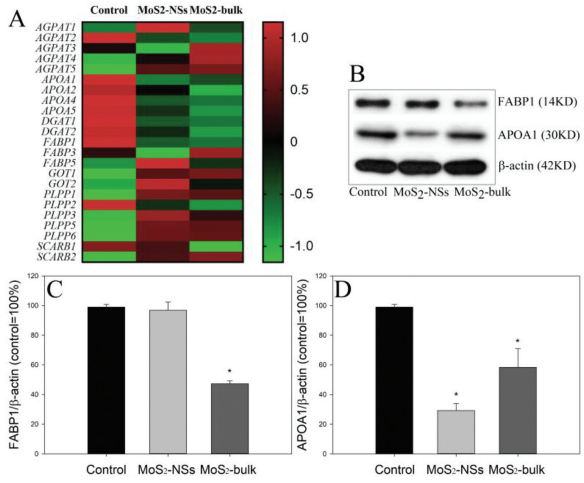

Fig. 3. The changes of key components in fat digestion and absorption (map04975). 3D Caco-2 spheroids were incubated with cell culture medium (control), 32 μg/mL MoS_2 NSs or MoS_2-bulk for 24 h. (A) a heatmap for key genes related with fat digestion and absorption was generated. (B) The bands of proteins, the unedited Western blotting images are in Fig. S15 (Supporting information). (C) The changes of protein levels of FABP1. (D) The changes of protein levels of APOA1. *, $P < 0.01$, compared with control, ANOVA.

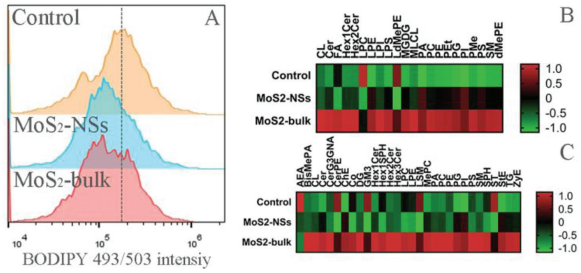

Fig. 4. The changes of lipid levels. 3D Caco-2 spheroids were incubated with cell culture medium (control), 32 μg/mL MoS_2 NSs or MoS_2-bulk for 24 h. (A) The dissociated cells were stained with BODIPY 493/503 for lipid droplets, and the changes of intensity of BODIPY 493/503 were determined. The changes of lipid profiles were determined under negative (B) or positive ion mode (C). Abbreviations for all lipid classes: AEA, *N*-acylethanolamine; BisMePA, bis-methyl phosphatidic acid; CL, cardiolipin; Cer, ceramide; CerPE, ceramide phosphoethanolamines; ChE, cholesterol ester; Co, coenzyme; DG, diglyceride; dMePE, dimethylphosphatidylethanolamine; FA, fatty acid; GM3, gangliosides; Hex1Cer, Hex2Cer, Hex3Cer, CerG3GNA, simple Glc series; Hex1SPH, glucosylsphingosine; LPC, lysophosphatidylcholine; LPE, lysophosphatidylethanolamine; LPI, lysophosphatidylinositol; LPS, lysophosphatidylserine; LdMePE, lysodimethylphosphatidylethanolamine; LSM, lysosphingomyelin; MePC, methyl phosphatidylcholine; MGDG, monogalactosyldiacylglycerol; MLCL, cardiolipin; PA, phosphatidic acid; PC, phosphatidylcholine; PE, phosphatidylethanolamine; PEt, phosphatidylethanol; PG, phosphatidylglycerol; PI, phosphatidylinositol; PMe, phosphatidylmethanol; PS, phosphatidylserine; SM, sphingomyelin; SPH, sphingosine; ST, sulfatide; StE, stigmasterol ester; TG, triglyceride; ZyE, zymosterol ester.

be noticed that decreased lipid levels could also be due to the alterations in other processes, such as lipid metabolism and storage, as we observed recently in carbon nanotube-exposed THP-1 macrophages [40,41], vascular smooth muscle cells [42] and hepatocytes [43]. But here we did not further test the influence of MoS_2 materials on other lipid processes. Recent studies showed that classical 2D materials such as graphene-based NMs could promote lipid peroxidation *in vitro* [44,45] or disturb lipid metabolism *in vivo* [44,46]. In addition, a recent study by using proteomics showed that graphene oxide elevated lipoprotein lipase, an enzyme crucial for lipid metabolism, in macrophages. This might in turn affect lipid accumulation, although the authors did not further investigate this possibility [21]. We recently reported that graphene oxide decreased lipid contents and most of the lipid classes in THP-1 macrophages [30]. The effects of other types of NSs on lipid metabolism were less investigated, but one study showed that graphene oxide slightly decreased lipid accumulation, whereas MoS_2, WS_2 and BN NSs significantly increased lipid accumulation in human adipose-derived mesenchymal stem cells. Based on these observations, the authors concluded that NSs could influence the stem cell growth and differentiation [47]. Thus, it is possible that NSs were capable to affect lipid accumulation.

Despite the overall decrease of lipid contents, it is interesting to see that most of the lipid classes were indeed increased by MoS_2 NSs or MoS_2-bulk. By analyzing lipidomics data, we found that MoS_2 materials only decreased 8 lipid classes in 3D Caco-2 spheroids, namely lysophosphatidylcholine (LPC), lysodimethylphosphatidylethanolamine (LdMePE), N-acylethanolamine (AEA), ceramide phosphoethanolamines (CerPE), gangliosides (GM3), lysosphingomyelin (LSM) and sulfatide (ST).

In addition, MoS_2 NSs was more potent to decrease the lipid classes compared with MoS_2-bulk (Figs. 4B and C). Recently we reported that lipid components in lung surfactant did not affect multi-walled carbon nanotube-induced lipid accumulation but completely changed lipid compositions in THP-1 macrophages [48]. Hence, besides traditional methods, it is still necessary to use omics-techniques to investigate the exact influences of NMs.

In summary, the present study showed that MoS_2 NSs or MoS_2-bulk did not induce cytotoxicity to 3D Caco-2 spheroids despite substantial internalization, confirming that MoS_2 materials are relatively low toxic materials. However, MoS_2 NSs as well as MoS_2-bulk materials significantly decreased nutrient transport and metabolism, particularly fat digestion and absorption. In addition, MoS_2 materials decreased lipid levels and 8 lipid classes in 3D Caco-2 spheroids. These results suggested a need to investigate the adverse effects of NMs by systemic methods, even if the NMs have little to no cytotoxicity. Considering the findings of this study, NMs based on biocompatible and biodegradable materials may be more suitable for biochemical applications [49,50].

Declaration of competing interest

The authors declare that they have no known competing financial interests or personal relationships that could have appeared to influence the work reported in this paper.

Acknowledgments

This work was financially supported by National Natural Science Foundation of China (No. 51803055), Natural Science Foundation of Hunan Province (No. 2019JJ50372), and Hunan Provincial Key Research and Development Program (No. 2018GK2062).

Supplementary materials

Supplementary material associated with this article can be found, in the online version, at doi:10.1016/j.cclet.2021.06.049.

References

[1] H. Qian, J. Wang, L. Yan, J. Bioresour. Bioprod. 5 (2020) 204–210.
[2] X. Pan, J. Ji, N. Zhang, M. Xing, Chin. Chem. Lett. 31 (2020) 1462–1473.
[3] V. Yadav, S. Roy, P. Singh, Z. Khan, A. Jaiswal, Small 15 (2019) 1803706.
[4] T. Liu, Z. Liu, Adv. Healthc. Mater. 7 (2018) 1701158.
[5] J. Kaur, M. Singh, C. Dell'Aversana, et al., Sci. Rep. 8 (2018) 16386.
[6] W. Chen, W. Qi, W. Lu, et al., Small 14 (2018) 1702737.
[7] W.Z. Teo, E.L.K. Chng, Z. Sofer, M. Pumera, Chem. Eur. J. 20 (2014) 9627–9632.
[8] S. Liu, Z. Shen, B. Wu, et al., Environ. Sci. Technol. 51 (2017) 10834–10842.
[9] J. Hao, G. Song, T. Liu, et al., Adv. Sci. 4 (2017) 1600160.
[10] L. Mei, X. Zhang, W. Yin, et al., Nanoscale 11 (2019) 4767–4780.
[11] S. CC, A. Anusri, C. Levna, A. PM, D. Lekha, J. Hazard. Mater. 385 (2020) 121624.
[12] L. Xu, J. Zhao, Z. Wang, Sci. Total Environ. 664 (2019) 536–545.
[13] X. Li, Y. Tang, C. Chen, D. Qiu, Y. Cao, Toxicol. Appl. Pharmacol. 382 (2019) 114758.
[14] S. Li, X. Zheng, C. Huang, Y. Cao, Chin. Chem. Lett. 32 (2021) 1567–1570.
[15] S. Li, H. Liu, Z. Zhou, Y. Cao, Toxicol. in Vitro 62 (2020) 104689.
[16] Y. Cao, J. Appl. Toxicol. 42 (2022) 4–16.
[17] R. Chen, J. Qiao, R. Bai, Y. Zhao, C. Chen, Anal. Bioanal. Chem. 410 (2018) 6051–6066.
[18] Y. Cao, S. Li, J. Chen, Toxicol. Mech. Methods 31 (2021) 1–17.
[19] J. Wang, J. Zhang, S. Li, et al., Food Chem. 331 (2020) 127360.
[20] S.P. Mukherjee, B. Lazzaretto, K. Hultenby, et al., Chem 4 (2018) 334–358.
[21] X. Yang, Y. Zhang, W. Lai, et al., Nanotoxicology 13 (2019) 35–49.
[22] N. Wang, H. Wang, C. Tang, et al., Int. J. Nanomedicine 12 (2017) 5941–5957.
[23] A.M. Jastrzębska, A. Szuplewska, T. Wojciechowski, et al., J. Hazard. Mater. 339 (2017) 1–8.
[24] M. Gu, Z. Dai, X. Yan, et al., J. Appl. Toxicol. 41 (2021) 745–754.
[25] J. Augustyniak, A. Bertero, T. Coccini, et al., J. Appl. Toxicol. 39 (2019) 1610–1622.
[26] S.L. Chia, C.Y. Tay, M.I. Setyawati, D.T. Leong, Small 11 (2015) 702–712.
[27] T. He, J. Long, J. Li, L. Liu, Y. Cao, Environ. Toxicol. Pharmacol. 56 (2017) 233–240.
[28] X. Feng, Q. Chen, W. Guo, et al., Arch. Toxicol. 94 (2020) 1915–1939.
[29] Y. Cao, Y. Gong, L. Liu, et al., J. Appl. Toxicol. 37 (2017) 1359–1369.
[30] Y. Luo, J. Peng, C. Huang, Y. Cao, Ecotoxicol. Environ. Saf. 199 (2020) 110714.
[31] S. Wang, J. Ma, S. Guo, Y. Huang, Y. Cao, NanoImpact 20 (2020) 100270.
[32] Y. Cao, J. Li, F. Liu, et al., Environ. Toxicol. Pharmacol. 46 (2016) 206–210.
[33] Z. Guo, N.J. Martucci, Y. Liu, et al., Nanotoxicology 12 (2018) 485–508.
[34] F. Moreno-Olivas, E. Tako, G.J. Mahler, Food Chem. Toxicol. 124 (2019) 112–127.
[35] J.W. Richter, G.M. Shull, J.H. Fountain, et al., Nanotoxicology 12 (2018) 390–406.
[36] Z. Chen, Y. Wang, X. Wang, et al., J. Appl. Toxicol. 38 (2018) 810–823.
[37] H. Türkez, M.E. Arslan, E. Sönmez, et al., Chem. Biol. Interact. 300 (2019) 131–137.
[38] J.H. Tian, J.S. Hu, F.C. Li, et al., Biol. Open 5 (2016) 764–769.
[39] Y. Luo, X. Wang, Y. Cao, Chem. Biol. Interact. 333 (2021) 109325.
[40] T. Yang, J. Chen, L. Gao, et al., Toxicol. Lett. 332 (2020) 65–73.
[41] Q. Yang, M. Wang, Y. Sun, et al., Chin. Chem. Lett. 30 (2019) 1224–1228.
[42] H. Yang, J. Li, C. Yang, H. Liu, Y. Cao, Toxicol. Appl. Pharmacol. 374 (2019) 11–19.
[43] C. Zhao, Y. Zhou, L. Liu, et al., Food Chem. Toxicol. 121 (2018) 65–71.
[44] Y. Kim, J. Jeong, J. Yang, et al., Toxicology 410 (2018) 83–95.
[45] S.P. Mukherjee, B. Lazzaretto, K. Hultenby, et al., Chem 4 (2018) 334–358.
[46] M. Li, J. Zhu, M. Wang, et al., Chemosphere 236 (2019) 124834.
[47] I.R. Suhito, Y. Han, D.S. Kim, H. Son, T.H. Kim, Biochem. Biophys. Res. Commun. 493 (2017) 578–584.
[48] J. Lin, Y. Jiang, Y. Luo, et al., J. Hazard. Mater. 392 (2020) 122286.
[49] P. Zheng, Y. Liu, J. Chen, et al., Chin. Chem. Lett. 31 (2020) 1178–1182.
[50] M. He, L. Yu, Y. Yang, et al., Chin. Chem. Lett. 31 (2020) 3178–3182.